Brief Communications

Primary Afferent Terminals Acting as Excitatory Interneurons Contribute to Spontaneous Motor Activities in the Immature Spinal Cord

Rémi Bos, Frédéric Brocard, and Laurent Vinay

Laboratoire Plasticité et Physio-Pathologie de la Motricité, UMR 6196, Centre National de la Recherche Scientifique, and Aix-Marseille Université, F-13402 Marseille cedex 20, France

Patterned, spontaneous activity plays a critical role in the development of neuronal networks. A robust spontaneous activity is observed *in vitro* in spinal cord preparations isolated from immature rats. The rhythmic ventral root discharges rely mainly on the depolarizing/excitatory action of GABA and glycine early during development, whereas at later stages glutamate drive is primarily responsible for the rhythmic activity and GABA/glycine are thought to play an inhibitory role. However, rhythmic discharges mediated by the activation of $GABA_A$ receptors are recorded from dorsal roots (DRs). In the present study, we used the *in vitro* spinal cord preparation of neonatal rats to identify the relationship between discharges that are conducted antidromically along DRs and the spontaneous activity recorded from lumbar motoneurons. We show that discharges in DRs precede those in ventral roots and that primary afferent depolarizations (PADs) start earlier than EPSPs in motoneurons. EPSP-triggered averaging revealed that the action potentials propagate not only antidromically in the DR but also centrally and trigger EPSPs in motoneurons. Potentiating GABAergic antidromic discharges by diazepam increased the EPSPs recorded from motoneurons; conversely, blocking DR bursts markedly reduced these EPSPs. High intracellular concentrations of chloride are maintained in primary afferent terminals by the sodium-potassium-chloride cotransporter NKCC1. Blocking these cotransporters by bumetanide decreased both dorsal and ventral root discharges. We conclude that primary afferent fibers act as excitatory interneurons and that GABA, through PADs reaching firing threshold, is still playing a key role in promoting spontaneous activity in neonates.

Introduction

Spontaneous movements are a ubiquitous feature of fetal and infant behavior. They provide signals that are important for the development of neurons and the assembly of networks (Petersson et al., 2003; Hanson et al., 2008). Spontaneous movements are still present after deafferentation (Waldenström et al., 2009) or spinal transection (Robinson et al., 2000), indicating that they are generated, at least to a large extent, within the spinal cord.

A robust spontaneous activity is commonly observed *in vitro* in spinal cord preparations isolated from immature vertebrates (Landmesser and O'Donovan, 1984; Nakayama et al., 1999; Ren and Greer, 2003; Yvert et al., 2004). They are characterized by ventral root (VR) discharges, which rely mainly on the depolarizing/excitatory action of GABA and glycine at early developmental stages (for a recent review, see Vinay and Jean-Xavier, 2008). In contrast, at later stages (e.g., birth) it is widely accepted that glutamate drive is primarily responsible for the rhythmic activity (Ren and Greer, 2003; Myers et al., 2005) and that GABA plays an inhibitory role (Jean-Xavier et al., 2007). In addition, rhythmic discharges mediated by the activation of $GABA_A$ receptors are recorded from dorsal roots (DRs) (Fellippa-Marques et al., 2000). The present study was aimed at identifying the relationship between discharges that are conducted antidromically along DRs and the spontaneous activity recorded from lumbar motoneurons (MNs). We found that GABA, through its depolarizing action on primary afferent terminals, promotes spontaneous motor activity in neonates.

Materials and Methods

Animals and surgical procedures. Experiments were performed on Wistar rats of either sex aged from P1 to P4 (P0 was defined as the first 24 h after birth). All surgical and experimental procedures conformed to the guidelines from the French Ministry for Agriculture and Fisheries, Division of Animal Rights. Animals were anesthetized by hypothermia, decerebrated at a postcollicular level, and eviscerated. A laminectomy was performed, and the spinal cord and roots were removed from sacral segments up to T8–T10. The preparation was then pinned down, ventral side up, in the recording chamber. Dissection and recording procedures were performed under continuous perfusion with saline solution as follows (in mM): 130 NaCl, 4 KCl, 3.75 $CaCl_2$, 1.3 $MgSO_4$, 0.58 NaH_2PO_4, 25

Received Jan. 4, 2011; revised April 28, 2011; accepted May 31, 2011.

Author contributions: R.B. and L.V. designed research; R.B., F.B., and L.V. performed research; R.B. and L.V. analyzed data; R.B., F.B., and L.V. wrote the paper.

This work was supported by the Christopher and Dana Reeve Foundation (Grant VB1– 0502-2 to L.V.), the French Agence Nationale pour la Recherche, and the French Institut pour la Recherche sur la Moelle épinière et l'Encéphale. This article is dedicated to the memory of James P. Lund (1942–2009), whose work inspired the present experiments. We are grateful to Dr. F. Clarac for his comments on the manuscript.

Correspondence should be addressed to Laurent Vinay, CNRS, Laboratoire Plasticité et Physio-Pathologie de la Motricité, 31 Chemin Joseph Aiguier, F-13402 Marseille cedex 20, France. E-mail: vinay@dpm.cnrs-mrs.fr.

DOI:10.1523/JNEUROSCI.0068-11.2011

 0270-6474/11/3110184-05$15.00/0

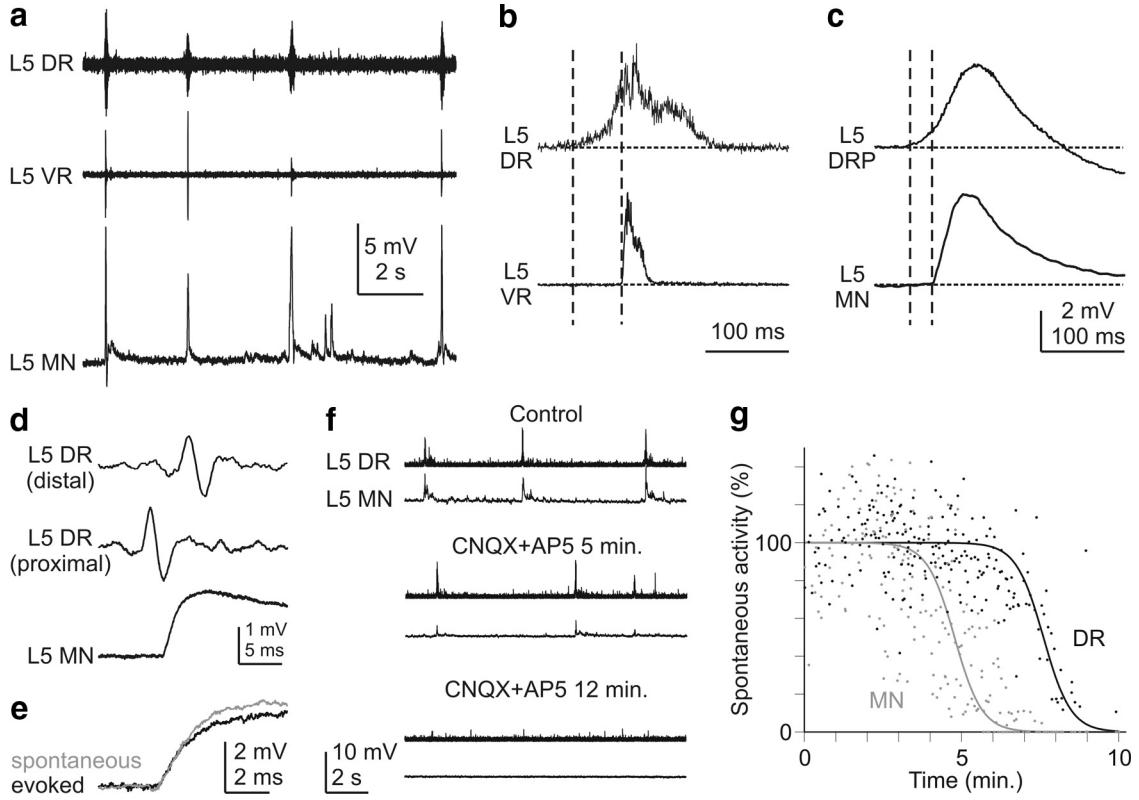

Figure 1. Discharges occur earlier in dorsal than in ventral roots. ***a***, Activities recorded from lumbar (L5) DRs and VRs, and MNs on the same side at P3. ***b***, Averages of DR and VR bursts (top and bottom, respectively; same experiment as in ***a***). Traces were rectified, the onset of VR burst was determined, and 300-ms-long sections of traces (starting 100 ms before and ending 200 ms after burst onset) were exported for averaging. Thirty consecutive bursts were considered. Note the 58 ms difference between burst onsets in DRs and VRs. ***c***, Averages of DRPs and EPSPs recorded from an MN in the same segment (L5). Similar procedure for trace averaging as in ***b***. EPSP onset was determined and 300-ms-long sections of traces (starting 70 ms before and ending 230 ms after EPSP onset) were exported for averaging. Seventy-three events were considered for analysis. Depolarization of primary afferents starts before EPSP onset (32 ms). ***d***, Two electrodes were placed in contact with the L4 DR (P3). Data recording was triggered by the EPSP recorded from ipsilateral L4 MN (averaging of 59 events). Action potentials propagated in a proximodistal direction with a conduction velocity of ~0.8 m/s. ***e***, Averages of EPSPs (same MN as in ***d***) occurring spontaneously (gray trace, $n = 59$) and evoked by electrical stimulation of the proximal DR at an intensity just above threshold (black trace, $n = 5$). ***f***, Spontaneous activity in DRs and MNs (P3) was progressively blocked by CNQX (10 μM) and DL-AP5 (50 μM). Note the larger reduction in MNs, compared with DRs, at 5 min. ***g***, Areas of the bursts (rectified traces) in DRs and PSPs in MNs at P2–P4 (five experiments averaged). Data are normalized to control condition before application of CNQX and DL-AP5 (time $t = 0$). Data were best fitted by nonlinear regression lines (one site competition equation; $r = 0.74$ and $r = 0.80$, respectively, for DRs and MNs).

$NaHCO_3$, and 10 glucose; oxygenated with 95% O_2-5% CO_2; pH adjusted to 7.4, at room temperature (22–24°C).

Recordings. Monopolar stainless steel electrodes were placed in contact with the roots and insulated with Vaseline. Spontaneous activity was recorded from DRs and VRs of L4–L5 segments. To record DR potentials (DRPs), DRs were cut ~2 mm away from the spinal cord and the central stump was incorporated in a suction electrode filled with normal saline. Signals were amplified, filtered (AC-coupled amplifiers; bandwidth: 70 Hz to 1 kHz and 0.1–100 Hz, respectively, for "en passant" and DRP recordings), digitized (Digidata 1200 interface, pClamp 9 software, Molecular Devices; sampling frequency of 1–30 kHz). Lumbar MNs were monitored intracellularly using glass microelectrodes filled with 2 M K-acetate (70–120 MΩ resistance) after the pia had been removed. Membrane potentials were recorded in the discontinuous current-clamp mode (Axoclamp 2B amplifier, Molecular Devices). Only neurons exhibiting a stable (15 min) resting membrane potential were considered for analysis.

Data analysis. The number of action potentials was counted by using a software voltage discriminator and a peak detector (pClamp9 software). Root recordings were rectified and integrated. To analyze the relationship among the different signals, some sessions were recorded in the "fixed-length events" acquisition mode of the pClamp software. Results are presented in the form of mean ± SEM. The statistical tests used are given in the text and figures legends (Prism 4 software, Graphpad).

Pharmacology. *Picrotoxin (PTX; 20 μM), diazepam (20 μM), bumetanide (10–20 μM), [(dihydroindenyl)oxy]alkanoic acid (DIOA; 30 μM) were obtained from Sigma. DL-2-Amino-5-phosphonopentanoic acid (DL-AP5) and 6-cyano-7-nitroquinoxaline-2,3-dione (CNQX) were purchased from Tocris Bioscience. DIOA was first prepared in DMSO (final concentration: 0.1%). All compounds were applied in the bath over 20–30 min, and their effects were considered 15–20 min after the onset of drug application. At this time, in all experimental conditions, the rhythm and pattern were always stable for several minutes.

Results

Discharges in DR occur before those in VR

Spontaneous activity was recorded from lumbar DRs in nearly all the preparations tested ($n = 40/42$). It consisted in bursts of action potentials separated by silent periods (Fig. 1*a*) (7.9 ± 0.46 bursts/min, $n = 42$ from P1 to P4; burst duration: 209 ± 9 ms, $n = 27$). Rhythmic discharges in VRs ($n = 39/42$) occurred in phase with DR bursts (Fig. 1*a*). Intracellular recordings from MNs revealed PSPs, even when no discharge was seen on the VR. A steady positive current was injected through the microelectrode to try to reverse the PSPs. Most MNs (22/26) exhibited excitatory PSPs (EPSPs could not be reversed) (Fig. 1*a*, bottom trace) that often triggered an action potential. EPSPs could be followed by IPSPs, which reversed toward hyperpolarization when the MN was steadily depolarized. In 4 of 26 MNs, only IPSPs were detected.

Bursts in VR lagged behind those recorded from the homonymous DR (Fig. 1*b*, average of 30 rectified bursts). The time delay

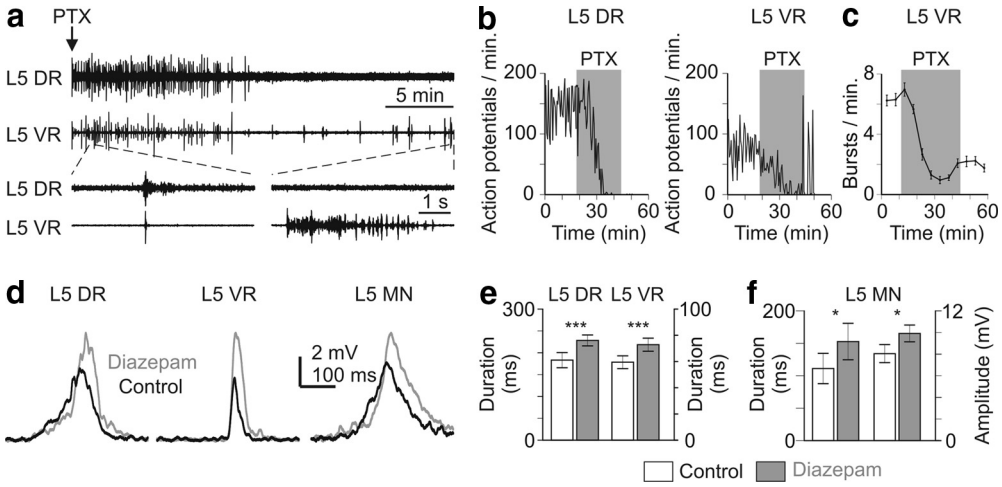

Figure 2. $GABA_A$ receptors play a key role in spontaneous activity. ***a***, Spontaneous bursting activities in DRs and VRs at P2 during the first 30 min following application of PTX (20 μM). Bottom traces are enlargements of top traces. ***b***, Number of action potentials per minute from L5 DR and VR before, during and after application of PTX (same experiment as in ***a***). ***c***, Frequency of spontaneous bursts in L5 VR (average of six experiments at P2–P4) before, during, and after application of PTX. ***d***, Averages of 21 bursts in DR (left trace) and VR (middle trace) and EPSPs in MN (right trace) recorded at P3 in control conditions (black traces) and after application of diazepam (gray traces, 20 μM, 30 min). DR and VR traces were rectified. Same procedure for averaging as in Figure 1*b*. ***e***, Significant increase in burst duration under diazepam for both DRs and VRs ($n = 12$ experiments; $p < 0.001$, paired *t* test). ***f***, Significant increase in both duration and amplitude of EPSPs under diazepam ($n = 6$; $p < 0.05$, Wilcoxon test).

ranged from 10 to 118 ms (mean: 46.8 ± 1.7 ms, $n = 150$ bursts in 15 preparations). This delay may be due to differences in the conduction velocity between primary afferent fibers and motor axons. To be rid of conduction delays, we recorded both DRPs and EPSPs from MNs. Primary afferent depolarizations (PADs), as indicated by DRPs, started earlier than EPSPs in MNs (Fig. 1*c*) (average lag: 17.4 ± 1.5 ms, $n = 165$ PADs and EPSPs analyzed in four preparations). EPSP trigger averaging revealed the presence of action potentials in the homonymous DR (Fig. 1*d*). Recording the same DR by means of two electrodes confirmed that these action potentials propagated antidromically from the spinal cord to the periphery (Fig. 1*d*) with a conduction velocity ranging from 0.8 to 1 m/s. The action potential recorded by the proximal electrode occurred before the EPSP onset (2.6 ms time lag). Interestingly, EPSPs evoked by electrical stimulation of the DR and those occurring spontaneously had similar slopes (Fig. 1*e*). These results demonstrate that discharges in DR propagate also centrally and have an effect on MNs. We added DL-AP5 (50 μM) and CNQX (10 μM) to the bath to block NMDA and non-NMDA receptors, respectively. This blocked spontaneous activity in both DRs and MNs within 10–15 min (Fig. 1*f*) ($n = 5$), confirming earlier observations (Ren and Greer, 2003) that excitatory amino acid transmission plays a key role in the rhythmic activity in neonates. However, the EPSPs in MNs decreased in amplitude and disappeared 2.5–3 min earlier than the bursts in DR (Fig. 1*f*, middle traces, *g*). These observations confirm that the activity is more robust in DRs than in MNs and raise the possibility that the DR discharges trigger motor activities by inducing the release of excitatory amino acids from primary afferents.

Blocking or potentiating $GABA_A$ receptor-mediated DR discharges modulate spontaneous motor activities

Because DR discharges are mediated by the activation of $GABA_A$ receptors (Fellippa-Marques et al., 2000), we applied picrotoxin (20 μM; $n = 6$) (Pflieger et al., 2002), a $GABA_A$ receptor antagonist. Antidromically propagated action potentials recorded from the DR disappeared within ~10–12 min ($p < 0.01$, paired *t* test) (Fig. 2*a*,*b*). Concomitantly, the number of action potentials recorded from the VR decreased markedly and the activity disappeared almost completely within ~15 min (Fig. 2*a*,*b*). In four of six preparations, a rhythm recovered that was characterized by longer periods (from 6.80 ± 0.75 to 1.55 ± 0.27 bursts/min; $p < 0.01$, paired *t* test) (Fig. 2*c*) and bursts (from 55 ± 8 to 234 ± 59 ms, $n = 4$; $p < 0.05$, paired *t* test) (Fig. 2*a*, compare bottom traces). Such rhythmic motor activities produced by disinhibited networks have been extensively studied (Bracci et al., 1996). In the remaining two of six preparations, no activity recovered.

We used diazepam ($n = 12$) to increase the opening of the $GABA_A$ receptor-gated chloride channel. In 10 of 12 preparations, a rhythmic bursting was observed in DRs in control conditions. As expected, applying this benzodiazepine increased the duration of the DR burst (Fig. 2*d*,*e*, left) (+31% in average for the 10 experiments; $p < 0.001$, paired *t* test). Surprisingly, VR bursts increased in both amplitude and duration (+34%, $p < 0.05$ and +24%, $p < 0.001$, respectively, paired *t* test) (Fig. 2*d*, middle traces, *e*, right histograms). In the remaining 2 of 12 preparations, no rhythmic discharges were recorded from DRs and VRs in control conditions; in those two cases, a rhythmic activity appeared on both roots under diazepam. To further investigate the effect of diazepam, we recorded EPSPs (identified by the fact that they could not be reversed when depolarizing the cell) from MNs. Those EPSPs occurring in phase with the DR discharges increased in both amplitude and duration (+26% and +44%, respectively; $n = 6$; $p < 0.05$, Wilcoxon test) (Fig. 2*d*, right traces, *f*). Altogether, these results reveal that blocking $GABA_A$ receptors or potentiating the effect of their activation results in a reduction or an increase in EPSPs, respectively.

Blocking sodium-potassium-chloride cotransporters NKCC1 affects both DR and VR discharges

Sodium-potassium-chloride cotransporters NKCC1 play a key role in maintaining $[Cl^-]_i$ high in primary afferent terminals (Alvarez-Leefmans et al., 1988). To block these chloride pumps, we used bumetanide, which has a greater affinity for NKCCs than for KCCs (Payne et al., 2003) and is usually used at concentrations <100 μM to be specific for NKCC1. Bumetanide at 10–20 μM markedly reduced DR discharges within a few minutes (Fig. 3*a*,*b*, left) ($p < 0.01$, Wilcoxon test; $n = 8$). Concomitantly, the

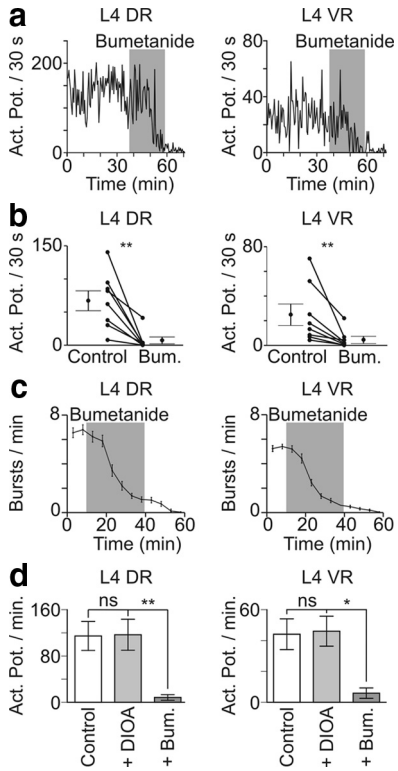

Figure 3. NKCC1 cotransporters play a key role in spontaneous activity. ***a***, Number of action potentials in L4 DR and VR before, during, and after the application of bumetanide (20 μM) in a single experiment at P3. ***b***, Significant decrease in the number of action potentials under bumetanide in both DR ($p < 0.01$, Wilcoxon test) and VR ($p < 0.01$). The data from eight experiments (P1–P4) and averages are plotted. ***c***, Burst frequency in L4 DR and VR ($n = 8$) before, during, and after bumetanide (10–20 μM). ***d***, Application of DIOA (30 μM) did not significantly affect the number of actions potentials in DR and VR ($p > 0.05$, one-wayANOVA, Tukey's post-test; $n = 5$). However, adding bumetanide to DIOA significantly decreased the number of action potentials in both roots ($p < 0.01$ and $p < 0.05$, respectively).

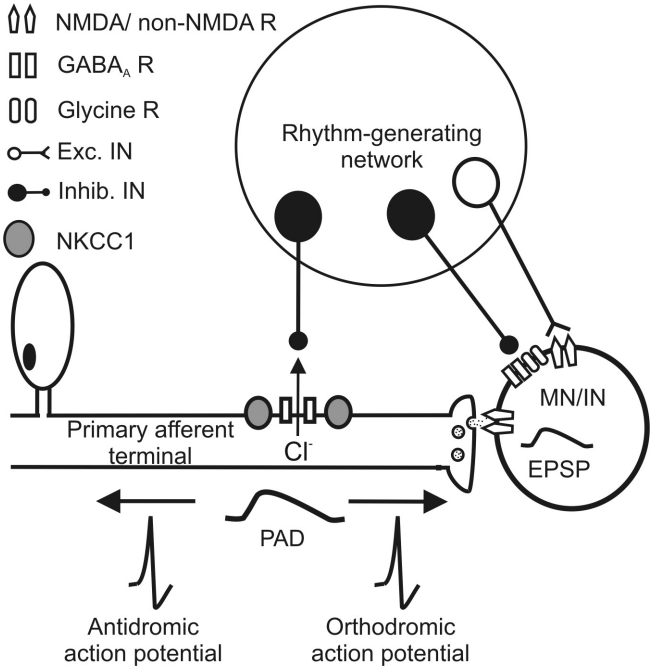

Figure 4. Connections that may account for the functional coupling between spontaneous dorsal and ventral root activities in the immature spinal cord. The network generating spontaneous activity activates GABAergic interneurons responsible for PADs. Action potentials that are triggered by PADs reaching firing threshold propagate both antidromically and orthodromically. The orthodromic volley generates EPSPs in MNs and/or premotor interneurons. In addition, MNs likely receive inputs from inhibitory and excitatory interneurons. The latter may account for the spontaneous bursting that recovers in the presence of picrotoxin. For the sake of clarity, the mechanisms responsible for chloride homeostasis in motoneurons (KCC2 and possibly NKCC1) are not included.

number of spikes recorded from the VR (Fig. 3*a*,*b*) ($p < 0.01$; $n = 8$) and the frequency of spontaneous bursts (Fig. 3*c*) ($p < 0.01$) decreased significantly under bumetanide. The effects on both roots were reversible, and some activity reappeared >1 h after washing out bumetanide. To further test whether the effects of bumetanide were due to a blockade of NKCC1, not KCC2, we applied DIOA (30 μM) to block the latter cotransporters (Boulenguez et al., 2010). DIOA affected neither the number of actions potentials in DRs and VRs (Fig. 3*d*) ($p > 0.05$, one-way ANOVA, Tukey's post-test; $n = 5$) nor the frequency of bursting. Adding bumetanide to DIOA markedly reduced DR and VR bursting (Fig. 3*d*) ($p < 0.01$ and $p < 0.05$, respectively).

Discussion

A robust bursting antidromic activity is recorded from lumbar DRs in the *in vitro* spinal cord preparation isolated from neonatal rats (see Results) (see also Kremer and Lev-Tov, 1998; Fellippa-Marques et al., 2000). The sensory fibers exhibiting antidromic discharges were not identified in the present study because, in contrast to adults, primary afferents cannot be characterized by their conduction velocities in neonates since they are nonmyelinated. However, the values that we calculated (0.8–1 m/s) fall in the upper range of the distribution of conduction velocities of afferent units at this age (Fitzgerald, 1987). Antidromic discharges were blocked by picrotoxin and bumetanide, demonstrating that GABA$_A$ receptors and NKCC1 cotransporters were involved. It is well established that GABA, through the activation of GABA$_A$ receptors, plays a major role in generating PADs (Rudomín et al., 1981). PADs rely on a high $[Cl^-]_I$, which is maintained by the chloride intruders NKCC1 cotransporters (Alvarez-Leefmans et al., 1988). When PADs are large enough to reach firing threshold, they trigger discharges that are antidromically conducted into peripheral nerves (Dubuc et al., 1985; Vinay and Clarac, 1999; Beloozerova and Rossignol, 2004).

Antidromic discharges were accompanied by bursts in VRs and/or subthreshold EPSPs in MNs. This may indicate that the rhythm-generating network activates both of the GABA interneurons responsible for PADs and MNs. However, we made the following observations, some of which at first sight appeared paradoxical. (1) The activities recorded from DR preceded those of their ipsilateral segmental VRs and PADs started earlier than EPSPs in MNs. (2) EPSP-triggered averaging revealed that the action potentials propagate not only antidromically in the DRs but also centrally and that they trigger EPSPs in MNs. In agreement with these observations, DR reflexes in group Ia afferents have been shown in cats not only to propagate distally but also to release transmitter centrally (and thus to evoke EPSPs in MNs) and even to cause large reflex discharges under certain experimental conditions (for review, see Willis, 1999; Eccles et al., 1961; Eccles and Willis, 1963). (3) Surprisingly, potentiating GABAergic antidromic discharges by diazepam increased the EPSPs recorded from MNs, and, conversely, blocking DR bursts by PTX markedly reduced these EPSPs, demonstrating that similar mechanisms are involved. These data are supported by an earlier study showing a bicuculline-sensitive increase in motoneuronal excitability associated with electrically evoked DR re-

flexes (Duchen, 1986). (4) Bumetanide at a low concentration to block NKCC1 cotransporters, suppressed both DR and VR bursts. Because IPSPs are still depolarizing from rest in neonatal rat MNs and are able to facilitate action potential generation when paired with EPSPs (Jean-Xavier et al., 2007), a possible explanation of the latter result could be that chloride homeostasis in MNs and possibly interneurons is involved. However, at such a low concentration, bumetanide has no effect on the reversal potential of IPSPs in neonatal rat motoneurons (Jean-Xavier et al., 2006), in agreement with the observation that NKCC1 does not appear to play a significant role in chloride homeostasis in those neurons at that age (Stil et al., 2009). In addition, DIOA, which shifts the reversal potential for IPSPs toward more positive values and should thereby enhance the facilitation of subthreshold EPSPs (Jean-Xavier et al., 2007), had no effect on VR bursts. The most likely explanation of our data is that rhythmically active GABAergic interneurons generate bursts of action potentials in DRs and that the central axon of primary afferents plays the role of a premotor interneuron carrying signals from the rhythm-generating network (Fig. 4), as shown in the trigeminal system (Kolta et al., 1995; Verdier et al., 2003). The observation that DR bursting persists whereas VR rhythmic activity ceases after cutting the mouse spinal cord lengthwise, thereby separating dorsal from ventral quadrants (Czéh and Somjen, 1989), supports this conclusion. The short delay between action potentials recorded from DRs and their postsynaptic effect on MNs (Fig. 1*d*) as well as the gradual disappearance of EPSPs when excitations were blocked (Fig. 1*g*) suggest that very few synapses are involved (likely no more than two).

To conclude, the present study demonstrates the existence of a functional compartmentalization of primary afferents in the spinal cord (for the trigeminal system, see Verdier et al., 2003; for the stomatogastric ganglion, see Coleman and Nusbaum, 1994). Antidromic activities in the peripheral branch block the input from the periphery and thereby contribute to the phasic gating that is observed during an episode of spontaneous movements (Waldenström et al., 2009), whereas the central branch provides additional excitation to the network and motoneurons.

References

Alvarez-Leefmans FJ, Gamiño SM, Giraldez F, Noguerón I (1988) Intracellular chloride regulation in amphibian dorsal root ganglion neurones studied with ion-selective microelectrode. J Physiol 406:225–246.

Beloozerova IN, Rossignol S (2004) Antidromic discharges in dorsal roots of decerebrate cats. II: studies during treadmill locomotion. Brain Res 996:227–236.

Boulenguez P, Liabeuf S, Bos R, Bras H, Jean-Xavier C, Brocard C, Stil A, Darbon P, Cattaert D, Delpire E, Marsala M, Vinay L (2010) Down-regulation of the potassium-chloride cotransporter KCC2 contributes to spasticity after spinal cord injury. Nat Med 16:302–307.

Bracci E, Ballerini L, Nistri A (1996) Spontaneous rhythmic bursts induced by pharmacological block of inhibition in lumbar motoneurons of the neonatal rat spinal cord. J Neurophysiol 75:640–647.

Coleman MJ, Nusbaum MP (1994) Functional consequences of compartmentalization of synaptic input. J Neurosci 14:6544–6552.

Czéh G, Somjen GG (1989) Spontaneous activity induced in isolated mouse spinal cord by high extracellular calcium and by low extracellular magnesium. Brain Res 495:89–99.

Dubuc R, Cabelguen JM, Rossignol S (1985) Rhythmic antidromic discharges of single primary afferents recorded in cut dorsal root filaments during locomotion in the cat. Brain Res 359:375–378.

Duchen MR (1986) Excitation of mouse motoneurones by GABA-mediated primary afferent depolarization. Brain Res 379:182–187.

Eccles JC, Kozak W, Magni F (1961) Dorsal root reflexes of muscle group I afferent fibres. J Physiol 159:128–146.

Eccles RM, Willis WD (1963) Presynaptic inhibition of the monosynaptic reflex pathway in kittens. J Physiol 165:403–420.

Fellippa-Marques S, Vinay L, Clarac F (2000) Spontaneous and locomotor-related GABAergic input onto primary afferents in the neonatal rat. Eur J Neurosci 12:155–164.

Fitzgerald M (1987) Cutaneous primary afferent properties in the hind limb of the neonatal rat. J Physiol 383:79–92.

Hanson MG, Milner LD, Landmesser LT (2008) Spontaneous rhythmic activity in early chick spinal cord influences distinct motor axon pathfinding decisions. Brain Res Rev 57:77–85.

Jean-Xavier C, Pflieger JF, Liabeuf S, Vinay L (2006) Inhibitory postsynaptic potentials in lumbar motoneurons remain depolarizing after neonatal spinal cord transection in the rat. J Neurophysiol 96:2274–2281.

Jean-Xavier C, Mentis GZ, O'Donovan MJ, Cattaert D, Vinay L (2007) Dual personality of GABA/glycine-mediated depolarizations in the immature spinal cord. Proc Natl Acad Sci U S A 104:11477–11482.

Kolta A, Lund JP, Westberg KG, Clavelou P (1995) Do muscle-spindle afferents act as interneurons during mastication? [letter; comment]. Trends Neurosci 18:441.

Kremer E, Lev-Tov A (1998) GABA-Receptor-independent dorsal root afferents depolarization in the neonatal rat spinal cord. J Neurophysiol 79:2581–2592.

Landmesser LT, O'Donovan MJ (1984) Activation patterns of embryonic chick hind limb muscles recorded in ovo and in an isolated spinal cord preparation. J Physiol 347:189–204.

Myers CP, Lewcock JW, Hanson MG, Gosgnach S, Aimone JB, Gage FH, Lee KF, Landmesser LT, Pfaff SL (2005) Cholinergic input is required during embryonic development to mediate proper assembly of spinal locomotor circuits. Neuron 46:37–49.

Nakayama K, Nishimaru H, Iizuka M, Ozaki S, Kudo N (1999) Rostrocaudal progression in the development of periodic spontaneous activity in fetal rat spinal motor circuits *in vitro*. J Neurophysiol 81:2592–2595.

Payne JA, Rivera C, Voipio J, Kaila K (2003) Cation-chloride co-transporters in neuronal communication, development and trauma. Trends Neurosci 26:199–206.

Petersson P, Waldenström A, Fåhraeus C, Schouenborg J (2003) Spontaneous muscle twitches during sleep guide spinal self-organization. Nature 424:72–75.

Pflieger JF, Clarac F, Vinay L (2002) Picrotoxin and bicuculline have different effects on lumbar spinal networks and motoneurons in the neonatal rat. Brain Res 935:81–86.

Ren J, Greer JJ (2003) Ontogeny of rhythmic motor patterns generated in the embryonic rat spinal cord. J Neurophysiol 89:1187–1195.

Robinson SR, Blumberg MS, Lane MS, Kreber LA (2000) Spontaneous motor activity in fetal and infant rats is organized into discrete multilimb bouts. Behav Neurosci 114:328–336.

Rudomín P, Engberg I, Jiménez I (1981) Mechanisms involved in presynaptic depolarization of group I and rubrospinal fibers in cat spinal cord. J Neurophysiol 46:532–548.

Stil A, Liabeuf S, Jean-Xavier C, Brocard C, Viemari JC, Vinay L (2009) Developmental up-regulation of the potassium-chloride cotransporter type 2 in the rat lumbar spinal cord. Neuroscience 164:809–821.

Verdier D, Lund JP, Kolta A (2003) GABAergic control of action potential propagation along axonal branches of mammalian sensory neurons. J Neurosci 23:2002–2007.

Vinay L, Clarac F (1999) Antidromic discharges of dorsal root afferents and Inhibition of the lumbar monosynaptic reflex in the neonatal rat. Neuroscience 90:165–176.

Vinay L, Jean-Xavier C (2008) Plasticity of spinal cord locomotor networks and contribution of cation-chloride cotransporters. Brain Res Rev 57:103–110.

Waldenström A, Christensson M, Schouenborg J (2009) Spontaneous movements: effect of denervation and relation to the adaptation of nociceptive withdrawal reflexes in the rat. Physiol Behav 98:532–536.

Willis WD Jr (1999) Dorsal root potentials and dorsal root reflexes: a double-edged sword. Exp Brain Res 124:395–421.

Yvert B, Branchereau P, Meyrand P (2004) Multiple spontaneous rhythmic activity patterns generated by the embryonic mouse spinal cord occur within a specific developmental time window. J Neurophysiol 91:2101–2109.